ELSEVIER

Contents lists available at ScienceDirect

### Journal of Molecular Liquids

journal homepage: www.elsevier.com/locate/mollig



## Revealing the role of hydrogen bonding interactions and supramolecular complexes in lignin dissolution by deep eutectic solvents



Qianwei Li<sup>a</sup>, Yuan Dong<sup>b</sup>, Karl D. Hammond<sup>a</sup>, Caixia Wan<sup>a,\*</sup>

- <sup>a</sup> Department of Biomedical, Biological, and Chemical Engineering, University of Missouri, Columbia, MO 65211, USA
- <sup>b</sup> School of Mechanical Engineering, Hangzhou Dianzi University, Hangzhou 310018, China

#### ARTICLE INFO

# Article history: Received 28 July 2021 Revised 29 September 2021 Accepted 4 October 2021 Available online 7 October 2021

Keywords:
Molecular dynamics
Deep eutectic solvents
Lignin
Cellulose
Lignocellulosic biomass
Pretreatment

#### ABSTRACT

Deep eutectic solvents (DESs) have great potential for lignocellulose valorization, especially in terms of lignin extraction and upgrading. It is important to understand the mechanisms involved in lignin dissolution in DESs in order to design solvents for biomass fractionation and extraction of property-tailorable lignin. Here, we use molecular dynamics simulations to gain mechanistic insights into lignin dissolution in DESs. Three DESs based on choline chloride with different hydrogen bond donors (HBDs) (i.e., ethylene glycol, formic acid, and lactic acid) are examined. The main intermolecular interactions in each DES as well as their interactions with lignin are identified. The association between lignin and cellulose in each DES is also investigated. The simulation results reveal that both the functional groups (i.e., hydroxyl group and carboxyl group) and the number of oxygen atoms in the HBD of a DES determine the characteristics of its hydrogen bonding network and the strength of its hydrogen bonding interactions with lignin. Ethylene glycol tends to form H-bonds with  $\alpha$ -OH in lignin and both lactic acid and formic acid prefer  $\gamma$ -OH in lignin. The average interaction energy between chloride ion and lignin is comparable to that between the HBD and lignin, indicating that the role of the anion in lignin dissolution is similar to that of the HBD in terms of thermodynamics. Molecular interactions between lignin and a DES are found to play a key role in dissociating lignin from cellulose. The number of aromatic rings of lignin on the cellulose in CCFA and CCLA are only 77% and 56% of that in CCEG. The insights gained in this study advance the understanding of lignin dissolution at the molecular level in DESs and provide guidance to design effective DESs for lignin extraction and valorization.

© 2021 Elsevier B.V. All rights reserved.

#### 1. Introduction

The use of lignocellulosic biomass in biorefining based on biochemical pathways entails pretreatment to break down lignocellulose complexes and facilitate the liberation of simple sugars as substrates for further conversion. In the context of a multistream biorefinery with improved profitability [1], a traditional biorefinery adopting current leading pretreatments (e.g., dilute acid, ammonia, steam explosion) would need to be reconfigured to generate high-value lignin-based coproducts while ensuring conversion of holocellulose-derived sugar streams. To this end, deep eutectic solvent (DES) pretreatment is emerging as an excellent option for biomass pretreatment in terms of improving cellulose digestibility, hydrolyzing hemicellulose, and extracting valorizable lignin [2].

\* Corresponding author.

E-mail address: wanca@missouri.edu (C. Wan).

DESs share many of the characteristics of ionic liquids (IL), such as low vapor pressure and thermal stability [3], but also offer advantages over ILs such as being non-toxic, biodegradable, easy to synthesize, and inexpensive [4]. DESs are eutectic mixtures of a hydrogen bond acceptor (HBA) and a hydrogen bond donor (HBD). The most common HBAs in DES pretreatment are quaternary ammonium salts with choline chloride (ChCl) [5]. There is more variability in the choice of HBD; common HBDs are based on polyols and carboxylic acids. The physicochemical properties of DESs can be tailored by rationally combining different constituents, which in turn define their utility for various applications. Prior studies have reported that different DESs can result in varying lignin extraction yields and various structures of the extracted lignin [2,6]. However, it remains challenging to predict the abilities of a particular DES to extract lignin due to our lack of understanding of the mechanisms of lignin extraction with DESs, so the selection of DESs for biomass fractionation has largely relied on trial-anderror so far. Consequently, there is a critical need for advancing our understanding of DES-lignin interactions to facilitate the

rational design of DESs for biomass fractionation and lignin extraction.

Lignin dissolution in a DES involves various inter- and intramolecular interactions, among which hydrogen bonding plays a key role. When hydrogen bonding interactions between a DES and lignin are too weak to compete with intermolecular hydrogen bonds (H-bonds) in lignin, it can result in insignificant dissolution of lignin from woody biomass. Adding an acid (e.g., AlCl<sub>3</sub>, H<sub>2</sub>SO<sub>4</sub>) or other additives can reconfigure molecular arrangements in a DES and strengthen its interactions with lignin. In the case of adding a Lewis acid (e.g., AlCl<sub>3</sub>) to a ChCl:glycerol DES, a density functional theory (DFT) study revealed that supramolecular complexes form between the acid and the DES [7], which serve as multisite bridging ligands for cleaving both H-bonds and ether bonds in lignocellulose complexes. For a ChCl-based DES with a HBD that serves as a Brønsted acid (proton donor), it was suggested that an acidic HBD (e.g., lactic acid) should contribute the majority of H-bonds with lignin rather than chloride anion [8].

Despite efforts made to understand DES-lignin interactions, the microscopic behavior of lignin in a DES and the roles of DES constituents in lignin dissolution remain unclear. Microscopic considerations are even more important when extending lignin dissolution to lignin separation from lignocellulose complexes. The first step in lignin extraction (delignification) is disruption of the strong associations between lignin and cellulose. One mechanism proposed for lignin–cellulose association is adsorption of lignin onto cellulose, which can be induced or influenced by the solvent [9]. DES pretreatment has been shown to dissolve lignin from lignocellulose complexes effectively, but the mechanisms of lignin–cellulose dissociation in a DES have yet to be fully elucidated. Fundamental understanding of lignin–cellulose interactions would provide guidance for efficient separation of lignin from lignocellulose complexes by a DES.

In this study, we used liquid-phase, all-atom molecular dynamics (MD) simulations to elucidate structural changes in lignin as well as lignin adsorption onto cellulose in a DES. Three DESs (i.e., ChCl:ethylene glycol, ChCl:formic acid, ChCl:lactic acid) that have all been reported to perform differently in biomass pretreatment [10–12] were selected to study the dissolution of lignin. Structural changes of lignin were characterized by the average solvent-accessible surface area (SASA), radius of gyration (Rg), and number of lignin–lignin hydrogen bonds. Lignin–DES interactions are characterized by the number of lignin–DES hydrogen bonds as well as the radial distribution function (RDF) and spatial distribution function (SDF). The number of contacts between lignin and cellulose was calculated to quantify the degree of lignin–cellulose association on both hydrophilic and hydrophobic surfaces of cellulose.

#### 2. Computational details

The three DESs used for our MD simulations were composed of choline chloride (CC) as an HBA and one of ethylene glycol (EG), formic acid (FA), or lactic acid (LA) as an HBD. These are hereafter referred to as CCEG, CCFA, and CCLA, respectively. The molar ratio of HBA to HBD was 1:2 for all three DESs. Atom identifiers for all compounds were defined based on the atoms' unique positions in the molecular skeletons, as shown in Fig. 1. For lignin, two model compounds were used, namely guaiacylglycerol- $\beta$ -guaiacyl ether (hereafter referred to as "GG dimer") (Fig. 2a), a commonly used lignin dimer [13–15], and Adler lignin (Fig. 2b), a softwood lignin model that includes all the common linkages in lignin [16–18]. An Adler lignin molecule contains 12 lignin monomers (G units) covalently bonded via seven  $\beta$ -O-4 linkages, one  $\beta$ -5 linkage, one 5–5′ linkage, one 5–0–4 linkage, and one  $\beta$ - $\beta$  linkage (Fig. 2b).

A crystalline cellulose-lignin complex was created to mimic lignin adsorption on the cellulose surface. The crystalline cellulose block was composed of 41 chains, each with a chain length of 10 monomers (i.e., glucose units). The crystalline cellulose-lignin block consisted of one crystalline cellulose molecule surrounded by 8 Adler lignin molecules. Two Adler lignin molecules were placed on the (100) face (hydrophobic surface) and the (010) face (hydrophilic surface) of one crystalline cellulose molecule. The cellulose-lignin bulk was placed at the center of the supercell (Fig. 2c). Geometries for all DES molecules were optimized via VAMP semi-empirical calculations in Materials Studio [19]. All parameters were left at their defaults. The partial charges of the choline cation in CCFA and CCLA, as well as partial charges on the atoms in formic acid, lactic acid, and GG dimer, were set equal to the Mulliken atomic charges derived from the VAMP calculations. Partial charges in ethylene glycol and the choline cation in CCEG were taken from the OPLSAA force field [20] and the work of Gilmore et al. [21], respectively. To determine the values of the partial charges in other DES molecules, we used the Mulliken charges from VAMP calculations in several independent simulations for each DES (data not shown). The charges yielding the best reproduction of the experimental density values were chosen for the rest of the simulations. Partial charges and geometries of Adler lignin and cellulose were based on a prior study by Rismiller et al. [18]. The initial geometry of the lignin–cellulose complex is shown in Fig. 2c. Except partial charges, force field parameters for choline chloride were derived from the DES-OPLS force field [22], and the parameters for HBDs, lignin models, and cellulose from OPLSAA force field [20].

Four MD simulation supercells were built for each DES: pure DES, DES-GG dimer, DES-Adler lignin, and DES-lignin-cellulose. Molecules were randomly placed with a gap (3 Å) between molecules using Moltemplate [23]. For the pure DES systems, 500 ChCl pairs and 1000 HBDs were included in the supercell. For the DES-GG dimer systems, 500 ChCl pairs, 1000 HBD molecules, and 120 lignin dimers were included. The total molecular weight of lignin in the box was 38440.8 g/mol with 2040 carbon atoms, and the GG dimer concentration in each DES solvent was 19-25 wt%. For the Adler lignin-DES systems, 500 ChCl pairs, 1000 HBD molecules, and 18 Adler lignin molecules were placed in the simulation box. The total molecular weight of the Adler lignin model compound was 39528 g/mol; each molecule contained 2080 carbon atoms, and the Adler lignin concentration was 13-17 wt%. Lignin concentrations in the simulations were chosen to be similar to those in experiments on lignin dissolution with DESs [24]. For DES-lig nin-cellulose systems, 500 ChCl pairs, 1000 HBD molecules, 8 Adler lignin molecules, and one crystalline cellulose molecule were included in the supercell (Fig. 2d).

Molecular dynamics (MD) simulations were carried out using LAMMPS [25]. Periodic boundary conditions were employed in all Cartesian directions. Long-range electrostatics were treated with a particle-particle-mesh (PPPM) solver with a relative error tolerance of  $10^{-5}$  and a cutoff of 10 Å. The 1–2 pairwise interactions (i.e., interactions between two directly bonded atoms) and 1-3 pairwise interactions (i.e., interactions between atoms separated by two bonds) were turned off for all specified pairs of atoms by setting the weights on the 1-2 and 1-3 pair-wise Lennard-Jones and Coulombic interactions to 0. To apply the same parameters for both intra- and intermolecular interactions [22]. the 1-4 intramolecular interactions were scaled by 0.5. The supercell was brought to equilibrium at T = 300 K using Parrinello-Rahman dynamics (fix npt); all three spatial dimensions were coupled in the barostat, and time constants of 100 and 1000 time steps were used for the thermostat and barostat, respectively. The pressure was set to 1 atm. Velocities of atoms were randomly assigned with a Boltzmann (Gaussian) distribution consistent with

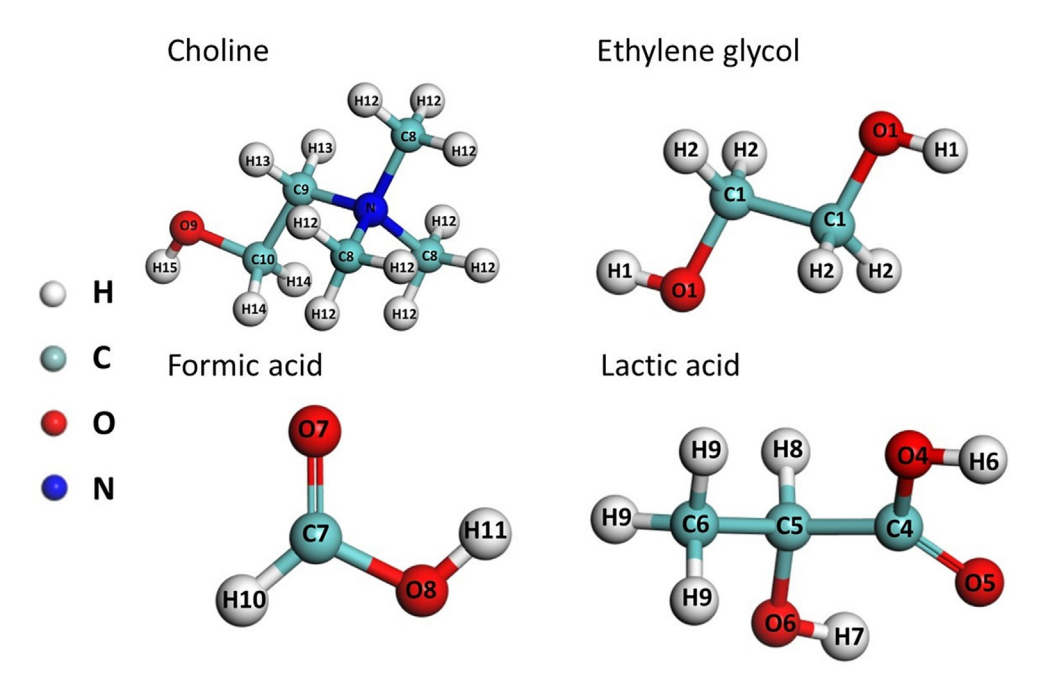


Fig. 1. Atom types assigned to choline cations and HBD molecules used in the MD simulations.

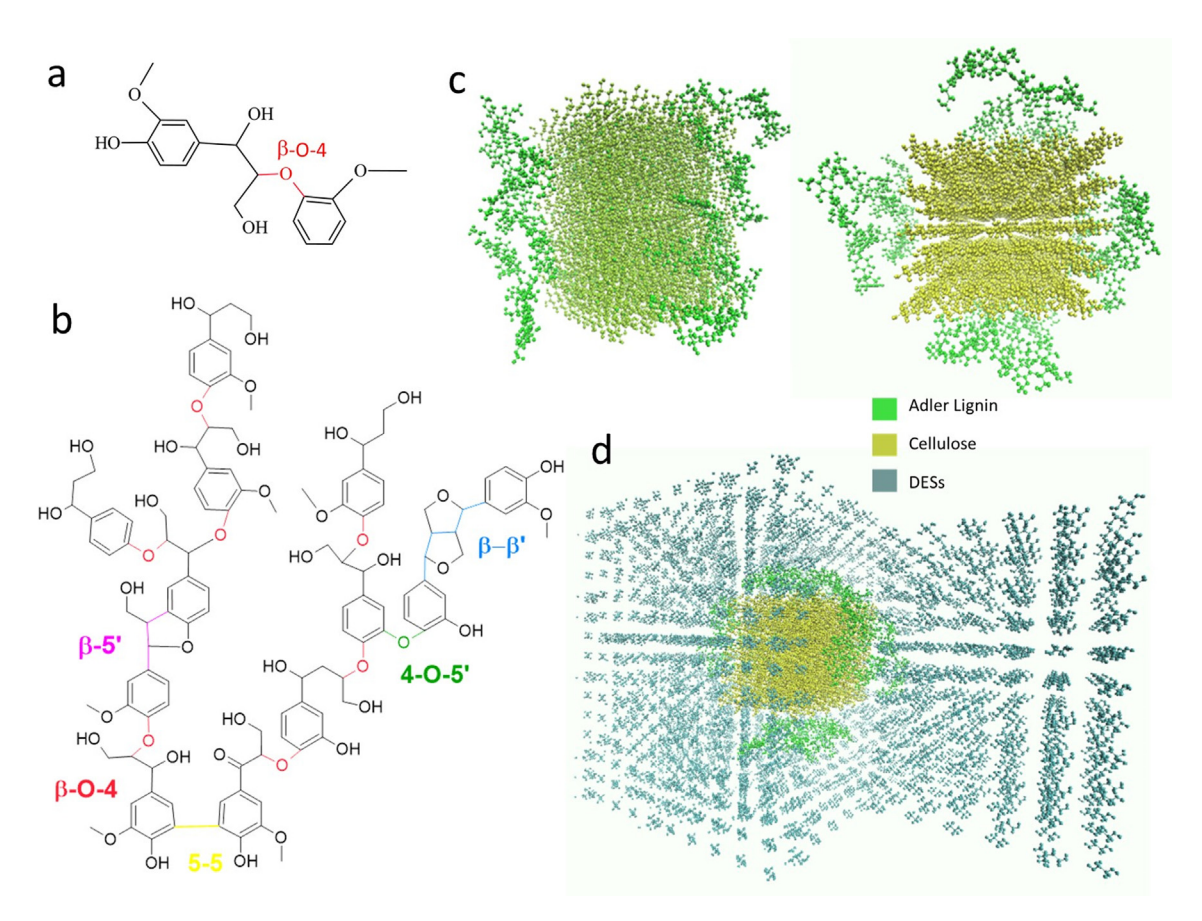


Fig. 2. (a) Guaiacylglycerol- $\beta$ -guaiacyl ether. (b) Adler lignin structure. (c) Initial geometry of lignin-cellulose bulk. (d) Initial geometry of lignin-cellulose-DES. Alder lignin was used for the simulation of lignin-cellulose interactions.

T = 300 K. Dynamics were run at an initial time step of 0.01 fs for 200,000 time steps to allow any unrealistically-close molecules to settle into near-equilibrium positions. The time step was increased from 0.01 to 0.1 fs after 200,000 steps, then to 1 fs after 200,000

more steps. The timestep was held constant at 1 fs for the rest of the simulation while the barostat and thermostat remain on.

Besides the above equilibration process, different strategies were used before or after the process to reduce the likelihood of unrealistically high forces due to non-physical molecular overlap. For Adler lignin–DES systems, energy minimization was first performed on the supercell before the equilibration process with relative tolerances of  $10^{-4}$  for energy and  $10^{-6}$  for force. For lignin–cellulose–DES systems, the initial temperature was set to 400 K and held there for 1 ns to accelerate the diffusion of solvent molecules. The temperature was then decreased to 300 K for at least 200 ps before analysis.

The output was recorded every 10,000 time steps by averaging 10 values sampled every 1000 timesteps. From the final coordinates after equilibration, five independent production runs with a total time of 1 ns each were computed for use in the structural characterization and analysis. A 200 ps trajectory with snapshots every 1 ps was used for further analysis. To analyze the molecular arrangement in the simulations, the radial distribution function (RDF) and number of H-bonds were calculated with VMD [26]. H-bonds were defined by the criterion that the distance between the donor (D) and acceptor (A) was less than 3.5 Å and the angle of  $\angle$  D—H A was less than 150°. The coordination number (CN) is the integral of the first peak of the RDF. The spatial distribution function (SDF) was calculated via Travis [27] and visualized with VMD. To characterize lignin structures, SASA and  $R_g$  were computed with VMD (using the commands "measure sasa" and "measure rgyr"). The radius of the probe is 1.4 Å in the calculation of the SASA. To quantify the degree of association between lignin and cellulose, the number of close contacts between cellulose and lignin (either for all atoms in lignin or for the center of mass (COM) of the aromatic rings in lignin) was calculated, with "close contact" defined as the distance between two atoms being 3 Å or less.

#### 3. Results

#### 3.1. Complex molecular interactions in DESs

The pure DES systems were simulated to identify the features of their molecular arrangements. The SDF, RDF, and the number of H-bonds were used to provide the detailed insights into the preferential positioning of chloride anions and oxygen atoms of the HBDs surrounding both choline cation and other HBD molecules in the solvents. The green, purple, and cyan blocks in Fig. 3 represent the most probable sites of chloride anion (in green), O1/O4/O8 in

HBD (in purple), and O6/O7 in HBD (in cyan), respectively. Fig. 3a-c shows that both chloride anions and oxygen atoms in HBD appear around the nitrogen atoms and oxygen atoms of choline cation. When the HBD is observed, the SDF shows that it is surrounded by molecules of the DES with different patterns (Fig. 3df). In CCEG, the strongest interaction is between chloride anion and the hydroxyl groups of ethylene glycol, according to the RDF (see Fig. S1 in the Supporting Information), which contributes 61% of the total H-bonds formed between choline chloride and ethylene glycol in the solvent. Fig. 3d depicts how chloride anion and ethylene glycol bind together via H-bonds and form the most common complex (referred to as a [Cl (EG)] complex) in this solvent. In CCFA, chloride anion also interacts with the hydroxyl group of formic acid, but the interaction is not as strong as that in CCEG. Rather, pair O8-O7 contributes most of the hydrogen bonds in CCFA, which are 160% more than that of pair Cl-O8. The O7 of formic acid (cvan in Fig. 3e) surrounds O8 from many directions, leading to a higher probability of forming hydrogen bonds with O8, while chloride (green in Fig. 3e) only gathers near the two hydrogen atoms. The significant interaction between O8 and O7 results in both intramolecular and intermolecular interactions of formic acid in CCFA. The intermolecular interaction is the selfaggregation of formic acid, which occurs between two carboxylic acid molecules, leading to the formation of a dimer [28]. A similar dimerization phenomenon was also reported for malonic acid in maline [29]. Similarly, the first three hydrogen-bonding types (O6···H···O4, O4···H···O5, and O6···H···O5) in CCLA all account for the inter- and intra-molecular interactions of three oxygen atoms (O4, O5, and O6) in lactic acid. This indicates that selfaggregation of lactic acid also happens in CCLA. As a result, lactic acid aggregates as dimers, trimers, and even tetramers, which has also been observed for lactic acid in water and methanol by vibrational absorption and vibrational circular dichroism spectroscopies [30]. The O6 of lactic acid (cyan in Fig. 3f) is convergent as a circle around O6, while the dominant atom around O4 is chloride. The high density around 06 in lactic acid implies that lactic acid self-aggregation mostly happens in the middle of the molecule, where O6-H is the main hydroxyl group contributing hydrogen atoms to the self-aggregation.

In short, DESs based on choline chloride have different solvent structures, depending on their hydrogen bonding networks. HBDs  $\,$ 

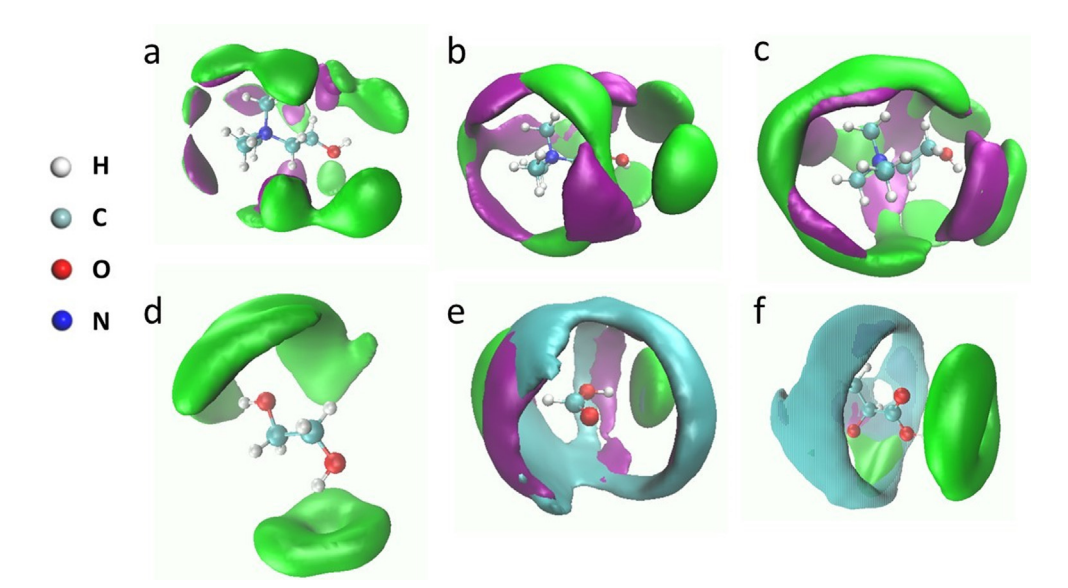


**Fig. 3.** Spatial distribution function (SDF) of chloride ions (green) and oxygen atoms (purple and cyan) of HBD centered around choline cation (top) and HBD (bottom). CCEG (a, d), CCFA (b, e), and CCLA (c, f) are shown. (For interpretation of the references to color in this figure legend, the reader is referred to the web version of this article.)

have different preferences in terms of hydrogen bonding interactions with chloride anion and the oxygen atoms of other HBD molecules. In CCEG, ethylene glycol tends to form a complex with chloride anions. In contrast, formic acid and lactic acid as HBDs tend to form more hydrogen bonds with themselves, leading to supermolecules, especially when the acid has more than two oxygen atoms. More types of bonded pairs can also be observed with lactic acid, as it has more than two functional groups. In such a case, carboxylic acid dimers and other oligomers would appear, which in turn restricts the mobility of chloride ion, leading to fewer hydrogen bonds between chloride anion and HBDs.

#### 3.2. Structural changes of GG dimer and alder lignin in DESs

Structural changes in lignin are characterized by the SASA and  $R_g$ , as depicted in Fig. 4. Larger values of the SASA and  $R_g$  indicate more open and extended structures of lignin. The SASAs of either lignin model in the three DESs are statistically similar, as is  $R_{\rm g}$ , because lignin aggregation is minimal. However, GG dimer and Adler lignin showed different behavior when encountering with three DESs due to their different mobility in the solvent and the different functional groups in lignin. For GG dimer, the average SASA of CCLA (587.8 Å<sup>2</sup>) is smaller than that of CCFA (602.2 Å<sup>2</sup>) and CCEG (604.97 Å<sup>2</sup>). This implies that GG dimer is more accessible to interact with CCEG than CCFA and CCLA at 300 K. For Adler lignin, it is observed that the average SASA in each DES system follows the order CCLA-AL (2618.992  $\text{Å}^2$ ) > CCEG-AL (2514.805  $\text{Å}^2$ -) > CCFA-AL (2435.845  $Å^2$ ), which is the opposite of the structural changes of GG dimer. Overall, most GG dimer molecules in DESs have larger SASA values than in the initial geometry, while Adler lignin followed the opposite trend. Fig. 4c and f illustrate how the average SASA correlates with lignin-lignin H-bonds. The average SASA of GG dimer decreased and more lignin-lignin Hbonds generates in CCEG and CCLA when the temperature was increased to 400 K. Meanwhile, the number of HBD-HBD and HBD-anion H-bonds decreased at 400 K relative to the number at 300 K (data not shown), which implies that for most intermolecular interactions, the H-bond distribution changes from 300 to 400 K. No clear correlation was found between the average SASA of GG dimer and its lignin-lignin H-bonds at either temperature (Fig. 4c). In contrast, the average SASA of Adler lignin shows a negative correlation with lignin-lignin H-bonds (Fig. 4f). In general, a lignin molecule with a more extended structure should have a larger SASA and fewer intramolecular H-bonds [31]. The negative correlation in Adler lignin exemplifies this phenomenon, indicating that intramolecular H-bonds are the main contributors to the total number of lignin-lignin H-bonds in Adler lignin. In contrast, for GG dimer, intermolecular H-bonds make up a larger portion of the total number of lignin-lignin H-bonds, especially at 300 K. The SASA of GG dimer increases relative to the initial geometry at 300 K, meaning that solvation decreases the strength of intramolecular interactions in lignin. When the temperature rises to 400 K, the SASA of GG dimer decreases and the number of lignin-lignin H-bonds increases. The decrease in SASA indicates that molecular interactions of GG dimer are mainly attributable to intramolecular H-bonds. Another interesting difference between the two lignin models is that Adler lignin has a broader distribution of SASA in DESs than GG dimer, which implies that its structural change is more sensitive to the lignin-solvent interactions.

#### 3.3. Interactions between chloride anion and lignin

Oxygen atoms in lignin are categorized in two ways in this work. In the first categorization, oxygen atoms are divided into three types, namely OA, OP, and OS. OA denotes two oxygen atoms in aliphatic hydroxyl groups of the lignin models, including  $\alpha\text{-OH}$  and  $\gamma\text{-OH}.$  OS denotes the three ether-like oxygen atoms of lignin, including oxygen atoms from methoxy groups and  $\beta\text{-O}$  in the  $\beta\text{-O}-4$  linkage. OP stands for the oxygen atom from aromatic hydroxyl groups of lignin. The second oxygen atom classification is based on the impact of the cleavage of lignin interunit linkages on hydrogen bonding interactions between a DES and lignin, where the oxygen atoms (or hydroxyl groups) of lignin are divided into four types:  $\alpha\text{-OH}, \gamma\text{-OH}, \beta\text{-O},$  and Ar-OH. The first three types are based on the carbon atoms in the aliphatic chains of lignin. Each Adler lignin molecule includes seven  $\alpha\text{-OH},$  ten  $\gamma\text{-OH},$  five Ar-OH, and seven  $\beta\text{-O},$  while each GG dimer has one of each type of oxygen atom.

Fig. 5 depicts the number of H-bonds between hydroxyl groups of lignin molecules and chloride anions of DESs at 300 K. The strength of hydrogen bonding is affected by the size of the lignin molecule and the presence of other molecules in the solution. GG

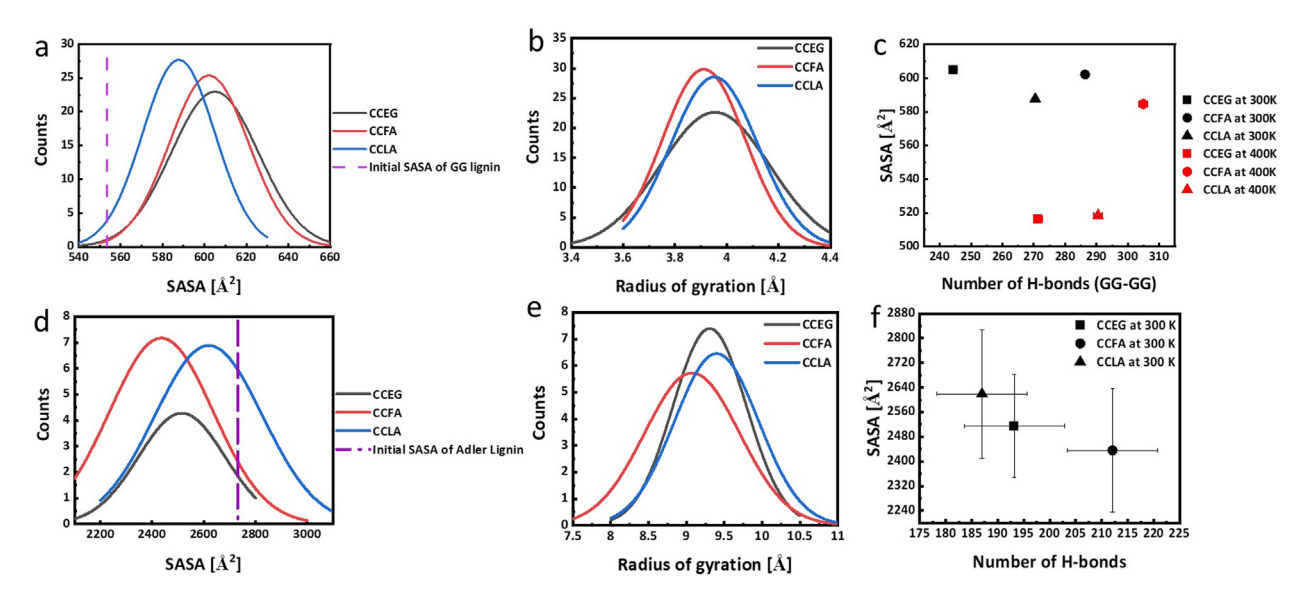


Fig. 4. Average solvent-accessible surface area (SASA) distribution, radius of gyration distribution for lignin, and correlation between the number of H-bonds for lignin–lignin and the average SASA in different DESs for GG dimer (a, b, c) and Adler lignin (d, e, f).

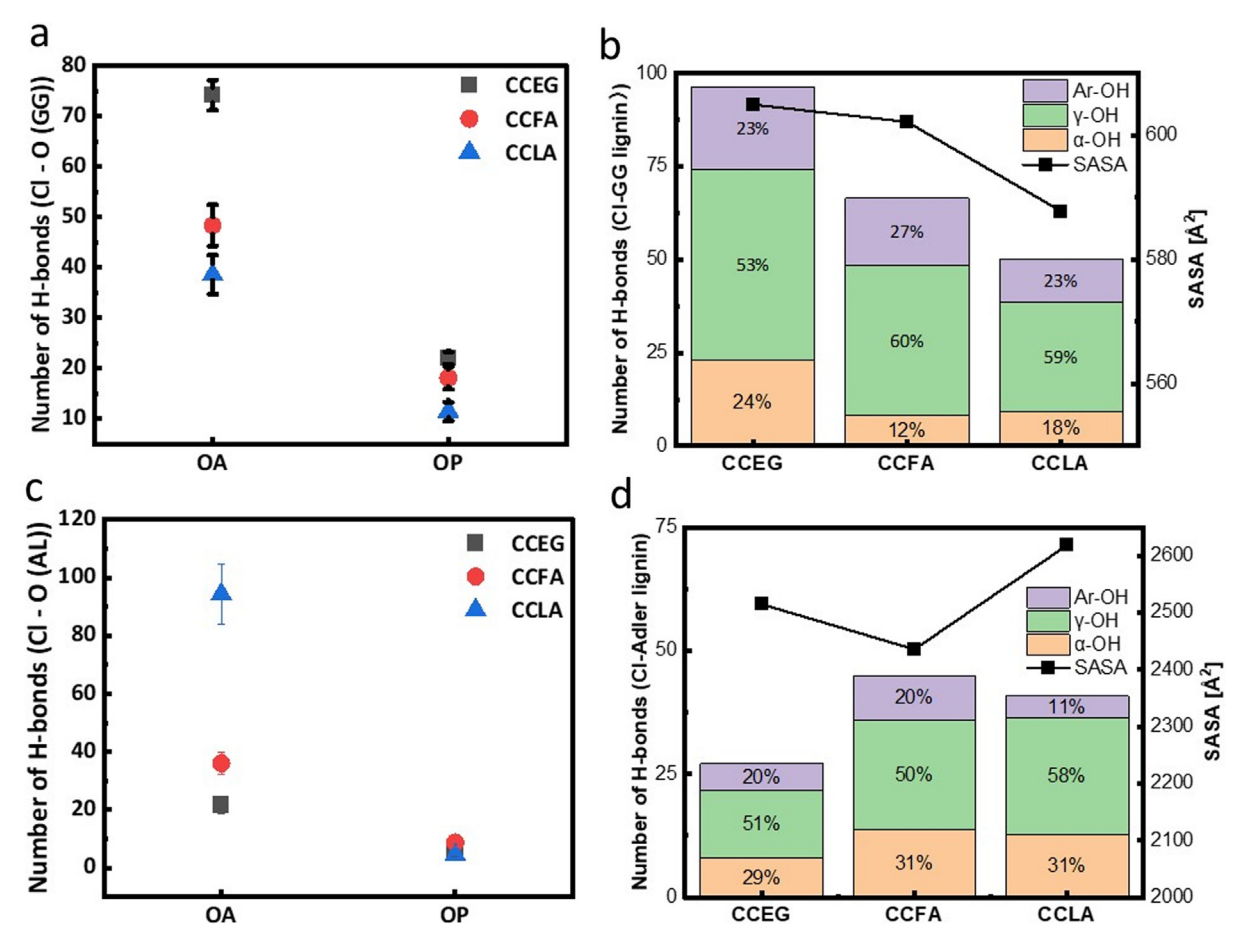


Fig. 5. Number of H-bonds between chloride ion and lignin at 300 K. (a, b) GG dimer and (c, d) Adler lignin.

dimer has a stronger bond with chloride ion than Adler lignin. To have a direct comparison of how the anion interacts with lignin, we normalized the effect of different amounts of the four types of oxygen atoms in the two lignin models by calculating the average number of H-bonds per oxygen atom for  $\alpha$ -OH,  $\gamma$ -OH, and Ar-OH. For CCEG-Adler lignin systems, each  $\alpha$ -OH,  $\gamma$ -OH, and Ar-OH would have 0.0627, 0.0764, and 0.0612H-bonds per molecule on average. The number of H-bonds between the anion and lignin is reduced by 73% from GG dimer to Adler lignin, and the anion's preference for  $\gamma$ -OH in Adler lignin also becomes less pronounced compared to that in GG dimer. The anion does not have enough strength to interrupt the intramolecular H-bonds in lignin in CCEG. On the other hand, compared to CCEG-Adler lignin systems, CCFA-Adler lignin systems have 1.7, 1.6, and 1.6 times more H-bonds for each α-OH, γ-OH, and Ar-OH, respectively, while CCLA-Adler lignin systems have 1.6, 1.7, and 0.8 times more, respectively. These results also indicate that  $\gamma$ -OH is the preferred site in lignin for chloride anion to interact with in a DES. CCEG favors hydrogen bonding between  $\gamma$ -OH and chloride anion compared to CCFA and CCLA. The preference for  $\gamma$ -OH is consistent across all six simulations. For GG dimer, more than half of the anions form H-bonds with  $\gamma$ -OH. The number of H-bonds between GG dimer and  $\gamma$ -OH increases with the average SASA of the dimer (Fig. 5b). The optimal site in lignin ( $\gamma$ -OH) for chloride anions in DESs is different from that  $(\alpha$ -OH) in 1-allyl-3-methylimidazolium chloride ionic liquids [32]. This suggests that chloride ions in DESs would have different roles in the cleavage of  $\beta$ -O-4 bonds compared to their role in ionic liquids. Moreover, though the Cl-OA RDF profiles of DESs show the peaks for two lignin model systems within the H-bonds' cutoff distances (Fig. S6), such peaks are less intense than those observed in ionic liquids [32]. The role of the anion in lignin dissolution is likely determined by the interaction of HBDs with lignin and the anion itself. In particular, the interaction between the HBD and lignin might determine whether the intermolecular H-bonds within lignin can be disrupted significantly and whether the anion can access more hydroxyl groups, especially  $\gamma$ -OH, in lignin. The interactions between the HBD and anion might determine the number of free anions available in the solvent that are not attached to HBD molecules. The effects of the HBD on various molecular interactions are further discussed in the rest of this section.

#### 3.4. Interactions between HBDs and lignin

The selection of an HBD is an important consideration for lignin dissolution in a DES, as it can play a key role in interacting with hydroxyl groups in lignin [8]. An HBD with more than two oxygen atoms tends to have stronger interactions with lignin, which is exemplified by the stronger H-bonds in CCLA than those in CCFA and CCEG. Among the three types of oxygen atoms (i.e., OA, OS, OP) in lignin, OA is the site that forms the strongest hydrogen bonds with the HBD across all three DESs (Fig. 6a and c); a similar trend exists for OA-anion interactions (Fig. 5a and c). For OP and OS, the CCFA and CCLA systems show similar numbers of H-bonds between carboxylic acids and lignin. However, CCEG shows that the number of H-bonds with the OP site of GG dimer is twice that found in either CCFA or CCLA. One possible explanation is the formation of [Cl (EG)]<sup>-</sup> complexes in CCEG, as discussed in later sections.

We find that lignin models with different structures can form different H-bond networks in a DES. As depicted in Fig. 6b and d,

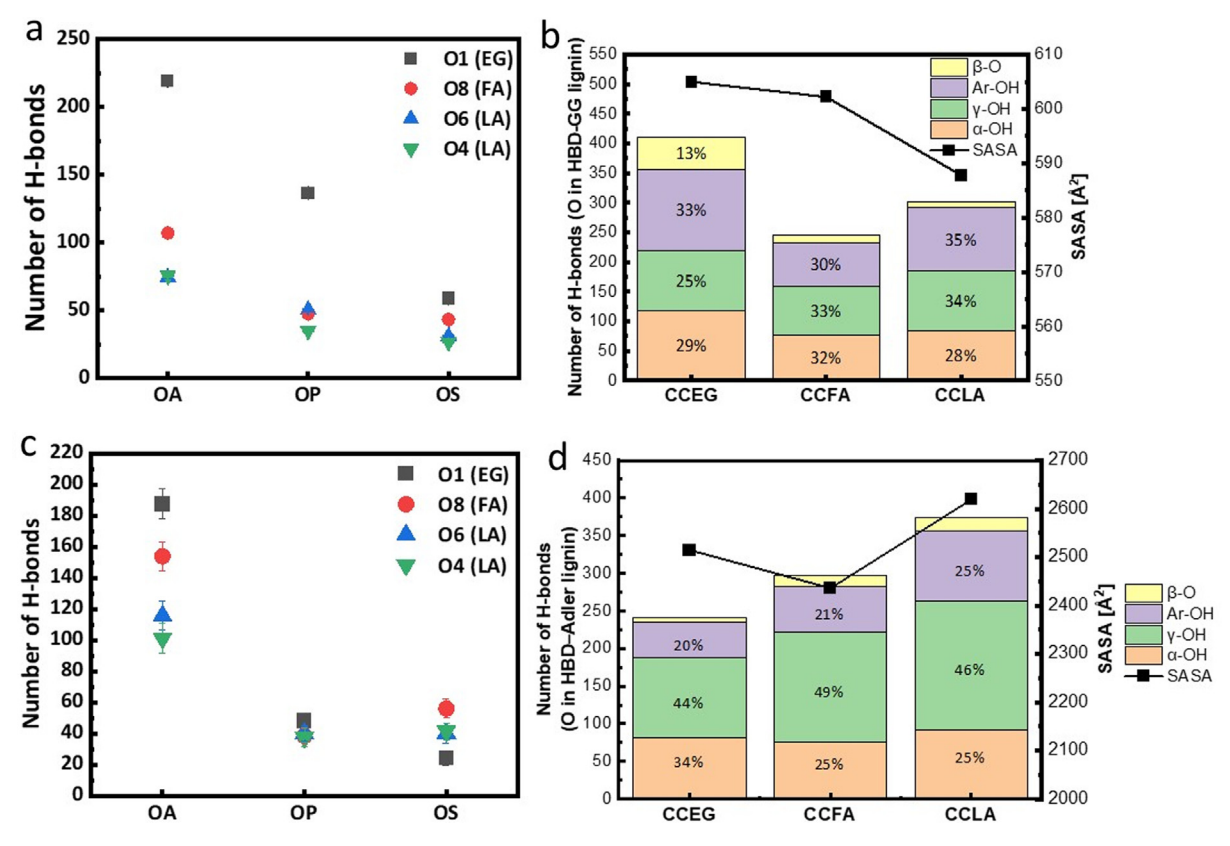


Fig. 6. Number of H-bonds of O in HBD-lignin at 300 K. (a, b) GG dimer and (c, d) Adler lignin. For clarity, data labels are hidden for values less than 5%.

the number of H-bonds at 300 K follows the order CCEG > CCLA > CCFA for GG dimer and CCLA > CCFA > CCEG for Adler lignin. The decrease in the number of H-bonds between CCEG and Adler lignin indicates that CCEG is not an effective solvent to dissolve lignin with large molecular weights. In contrast, the affinity of CCFA and CCLA to Adler lignin is strong. The different associations between the DES and lignin in the simulated systems should be related to the capability of a particular DES to disrupt inter-/ intra-molecular H-bonds in lignin molecules, which can determine that DES's effectiveness for lignin dissolution and depolymerization. Like the anion, HBDs also have their own preferred sites of interaction with lignin. A particular HBD could serve as a proton donor to attack  $\alpha$ -OH and  $\gamma$ -OH, which would cause the elongation of the C-O bonds. Based on the average number of H-bonds for each oxygen atom in lignin molecules (Fig. 6b), different HBDs show different abilities to attack  $\alpha$ -OH and  $\gamma$ -OH. Ethylene glycol molecules attack  $\alpha$ -OH more readily than carboxylic acids, and the proportion of H-bonds associated with  $\alpha$ -OH (35.5%) in Adler lignin is even higher than that in GG dimer (29%). Formic acid and lactic acid form more H-bonds with γ-OH than ethylene glycol, and the number of these H-bonds increases when encountering Adler lignin rather than GG dimer. The average proportion of H-bonds per oxygen atom for  $\gamma$ -OH is 36.6% for formic acid and 32.9% for lactic acid. The ratio of H-bonds with  $\alpha$ -OH to H-bonds with  $\gamma$ -OH is 1:1 for GG dimer and 7:10 for Adler lignin. The number of H-bonds between oxygen atoms in the HBD and  $\gamma$ -OH in Adler lignin increased markedly in CCFA (by 80.3%) and CCLA (by 68.5%) compared to the numbers of H-bonds for GG dimer. Such increases reveal the importance of the abundance of  $\gamma$ -OH in lignin on the lignin-DES interactions.

The propensity of HBDs to interact with the hydroxyl groups of lignin relates to the complexes formed in the solvents. As men-

tioned previously, carboxylic acid dimers appear in CCFA and CCLA, while the [Cl (EG)] $^-$  complexes are more common in CCEG. Two major differences among the complexes in the three DESs are the sizes of supramolecular assembly and available protons. Carboxylic acid dimers have more protons available than [Cl (EG)] $^-$  complexes, as the protons in carboxyl groups can easily dissociate from the dimers. On the other hand, carboxylic acid dimers, especially lactic acid dimers with larger supramolecular sizes than the polyol complexes, might occlude oxygen atoms on carboxyl groups from their interactions with the hydroxyl groups in lignin. In general,  $\gamma$ -OH is farther away from the aromatic rings of lignin than  $\alpha$ -OH and  $\beta$ -O-4, making it more accessible to the carboxylic acid dimers.

We next analyze how structural changes in lignin are governed by molecular interactions in a DES. Unlike Adler lignin, which has many branches and a complex structure that obstructs visualization, GG dimer is more suitable to visualize how the anion and oxygen atoms in HBDs surround the lignin molecules. Via observing GG dimer in the SDF, we can infer how the HBD and the anions in the DES alter the dimer morphology by interacting with those sites in the dimer. The favorable sites for H-bonding with chloride anion (green) and the oxygen atoms of HBDs (purple and cyan) around GG dimer are shown in Fig. 7. The chloride anions in the three DESs are mainly found surrounding the hydroxyl groups of GG dimer, which is consistent with the coordination numbers and numbers of H-bonds in Fig. 5a and b. The accumulation patterns of HBDs around a GG dimer show strong correlations with the HBD-HBD and HBD-anion interactions that are common in a DES. For CCEG, the spatial distribution of the oxygen atoms of ethylene glycol overlaps with the area occupied by the anions in CCEG. Such overlap can also be found in the SDF centered on the choline cation of pure CCEG, as shown in Fig. 3a, which is evidence that a massive amount of [Cl (EG)] complexes form in CCEG. Therefore,

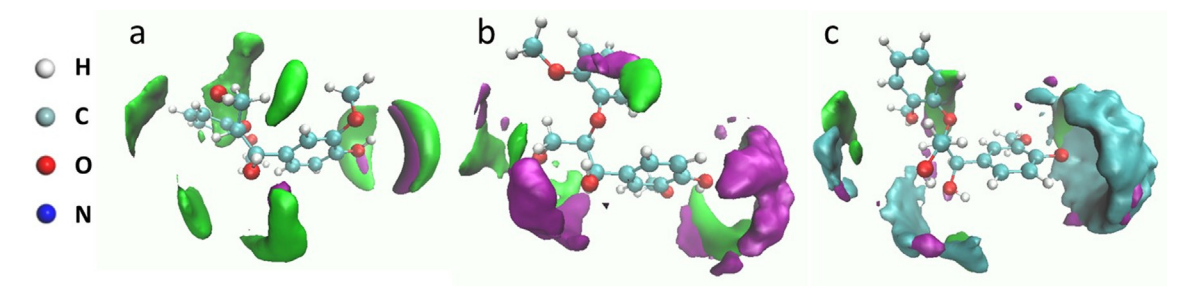


Fig. 7. Spatial distribution function (SDF) of chloride ions (green) and oxygen atoms (purple, cyan) of HBD centered around GG dimer. (a) CCEG, (b) CCFA, and (c) CCLA. (For interpretation of the references to color in this figure legend, the reader is referred to the web version of this article.)

GG dimer is more likely to interact with [Cl (EG)]<sup>-</sup>. The complexes primarily appear around the OP in GG, which is consistent with the high number of H-bonds found between OP and O1 in Fig. 6a. The strong hydrogen bonding interaction between Ar-OH and the [Cl (EG)] complexes can stretch the GG molecules to form an extended structure. The appearance of [Cl (EG)] complexes around  $\alpha$ -OH is also evident in Fig. 7a. In contrast to CCEG, the oxygen atoms in the HBDs of CCFA and CCLA primarily accumulate around  $\gamma$ -OH and Ar-OH. The proportions of H-bonds formed with Ar-OH,  $\alpha$ -OH, and  $\gamma$ -OH are not significantly different in CCFA (Fig. 6b). This observation indicates that the hydrogen bond strengths associated with those three sites should be comparable, and the elongation of the GG molecules due to hydrogen bonding should be similar among the three sites. However, the average SASA of GG is much lower in CCLA than in CCEG and CCFA. The local arrangement of the HBDs could be responsible for such a difference.

In CCFA, both the anion (green) and O8 (purple) in formic acid show up in an area closed to the OP (Fig. 7b), but their distributions do not overlap with each other. This arrangement allows the other GG molecules to form intermolecular H-bonds, which would contribute to a more open structure of GG. However, in CCLA, the H-bonds between lactic acid and lignin are equally likely to be formed around Ar-OH and  $\gamma$ -OH. The H-bonds between lactic acid and Ar-OH cause the OP in GG mostly to be bound to O6 in lactic acid, causing GG molecules to be less likely to make contact with one another.

The H-bonds between lactic acid and  $\gamma$ -OH can also promote the folding of lignin molecules. On one hand, GG might tend to self-aggregate into a folded structure due to the small molecular size. On the other hand, such an arrangement would be beneficial for a larger lignin molecule with more branches such as Adler lignin because the solvent complexes can penetrate into the low-density regions of the branches and prevent the branches from interacting with one another.

To gain a better understanding of the thermodynamics of lignin dissolution, we calculated the interaction energy between anion/ HBD and lignin molecules. As depicted in Fig. 8, pairwise interactions and long-range Coulombic forces almost equally determine the anion-lignin interaction energy for Adler lignin, while pairwise interactions contribute more for GG dimer. Pairwise interactions also contribute most of the HBD-lignin interaction energy for both GG dimer and Adler lignin. The interaction energy between HBD and Adler lignin is consistent with the number of H-bonds (Fig. 6b). The energy between HBD and GG dimer has an opposite trend for the number of H-bonds in CCLA and CCEG. Moreover, formic acid and lactic acid show similar interaction energies for both GG and Alder lignin molecule, while ethylene glycol prefers GG dimer. This indicates that besides hydrogen bonding, other molecular forces such as van der Waals forces would also contribute to the HBD-lignin interaction especially for a small lignin

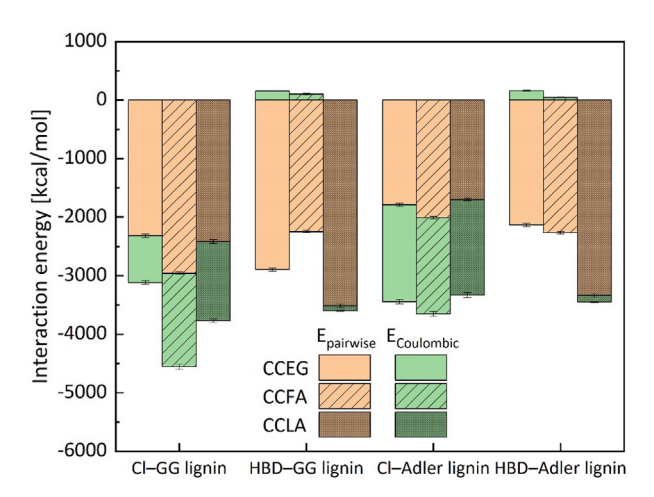


Fig. 8. Interaction energy (pairwise and long-range Coulombic) between Cl/HBD and lignin.

molecule. The difference in HBD-lignin interaction energy among the three DESs can be linked to the strength of the HBD-lignin interaction (Fig. 6a and b). The type of HBD can also affect the strength of anion-lignin interactions, with the highest interaction energy being observed with CCFA.

#### 3.5. Interactions between DES and lignin-cellulose bulk

Lignin–cellulose association was analyzed to understand the adsorption of lignin onto cellulose in a DES. Fig. 9 shows snapshots of how lignin was finally attached onto the surface of a cellulose chain. In general, the adhesion between cellulose and lignin is caused by lignin–cellulose hydrogen bonding interactions and influenced by the parallel orientation of the stacking structure between the aromatic rings of lignin and the glucopyranose rings of cellulose [33]. Thus, two main metrics, namely the number of H-bonds and the number of close contacts, were considered to quantify the adsorption behavior of lignin on cellulose.

Different types of molecules locating in the first solvation shell of the cellulose bulk are shown in Fig. 10a. Both the number of choline ions and lignin molecules surrounding the cellulose bulk follow the same order of CCEG > CCFA > CCLA. In CCLA, cellulose even shows a greater tendency to interact with lactic acid rather than other components in the system. This phenomenon can be interpreted in two aspects. On one hand, the close contacts between the HBD and cellulose is closely related to the number of atoms in the respective HBD. Apparently lactic acid, which has more atoms, should have more close contacts within the same distance. On the other hand, it implies that LA, which better attracts lignin, tends to be adsorbed onto the cellulose surface. The interactions between chloride anion and cellulose are relatively weak,

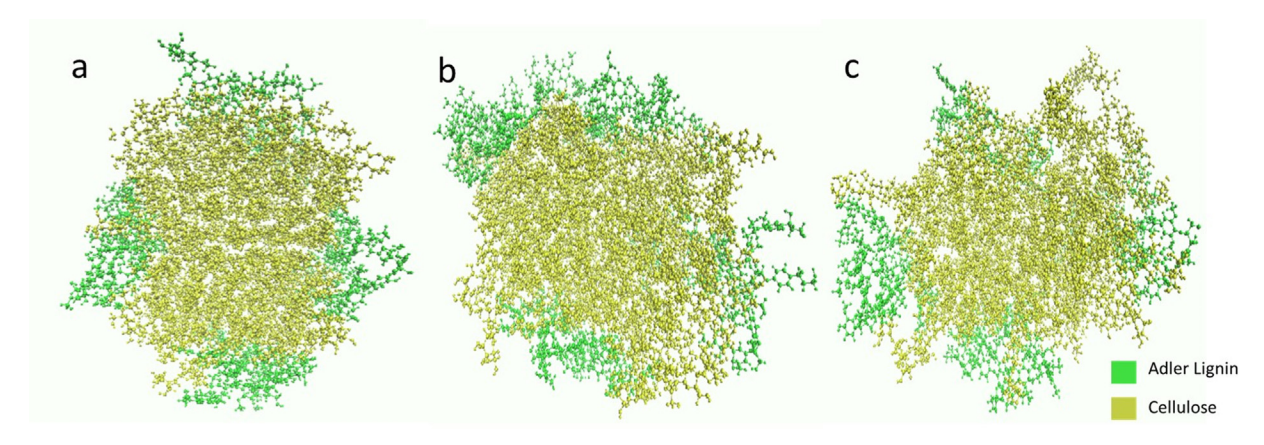
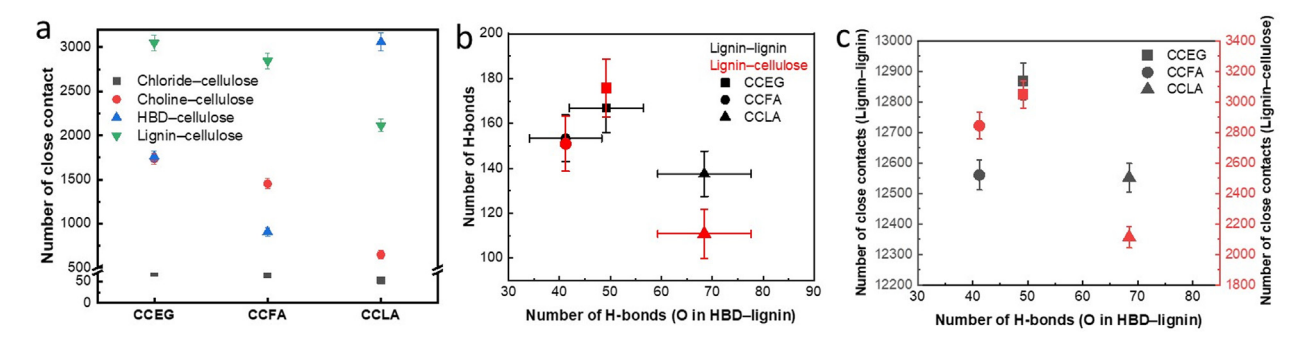


Fig. 9. Visual representations of the final configurations of the lignin–cellulose bulk in deep eutectic acid that used (a) ethylene glycol (EG), (b) formic acid (FA), and (c) lactic acid (LA).



**Fig. 10.** (a) Number of close contacts of molecules on the cellulose in the three DESs, (b) the correlation between the number of H-bonds and the number of H-bonds in HBD-lignin, and (c) the correlation between close contacts of lignin–lignin (black)/lignin–cellulose (red) and the number of H-bonds in HBD-lignin. (For interpretation of the references to color in this figure legend, the reader is referred to the web version of this article.)

with an average of 16 H-bonds between chloride and cellulose in each system (Fig. 10a). For H-bonds between lignin and the HBD, lignin forms the most hydrogen bonds with lactic acid, followed by ethylene glycol and formic acid (Fig. 10b). In contrast, the numbers of H-bonds in both lignin–lignin and lignin–cellulose follow the order CCEG > CCFA > CCLA (Fig. 10b). In particular, 89 H-bonds in lignin–cellulose are present in the initial configuration. When the system reaches equilibrium, the H-bonds in lignin–cellulose in CCEG, CCFA, CCLA increase by 98%, 70%, and 24% compared to the initial number, respectively. This further confirms that hydrogen bonding between the HBD and lignin can interrupt the intramolecular hydrogen bonding network of lignin.

The number of H-bonds in lignin-cellulose is roughly equal to that in lignin-lignin in CCEG and CCFA but lower in CCLA. These results indicate that there is a competition for H-bonds among cellulose, HBDs, and lignin. H-bonds in lignin-lignin and lignin-cellulose contribute to biomass recalcitrance. Overall, CCLA can disrupt the most H-bonds in lignin-lignin and lignin-cellulose, while CCEG shows the least potential. However, when we compare CCFA and CCEG, it is interesting to find that though FA forms fewer H-bonds with lignin than EG, the H-bonds in lignin-cellulose as well as lignin-lignin are reduced in CCFA. Such a finding may indicate that carboxylic-acid-based DESs have higher efficiencies in extracting lignin from cellulose compared to polyol-based DESs.

Atom-atom close contacts were also calculated to elucidate further how lignin molecules interact with the cellulose surface (Fig. 10c). The number of cellulose–lignin close contacts was also used to quantify the cellulose–lignin aggregation in another study [34]. The reduced number of close contacts between atoms of lignin and cellulose in CCLA confirmed the ability of lactic acid to

weaken the H-bonds between lignin and cellulose. Although formic acid does not show a similar ability, it has an ability comparable with lactic acid to reduce the number of close contacts of atoms within lignin (Fig. 10c). Moreover, Fig. 11 quantifies the dissociation between cellulose and lignin in a DES based on the number of close contacts between the COM of the aromatic rings of lignin and the atoms of cellulose. CCEG, CCFA, and CCLA have 50%, 38.5%, and 28%, respectively, of their aromatic rings (on a basis of 96 aromatic rings in total for each system) in close contact with the cellulose surface. Both measurements reveal that CCLA is more effective in dissociating lignin molecules from the surface of cellulose than the other two DESs.

As surface chemistry is a decisive factor for cellulose's affinity to lignin, we also investigated both hydrophobic and hydrophilic sur-

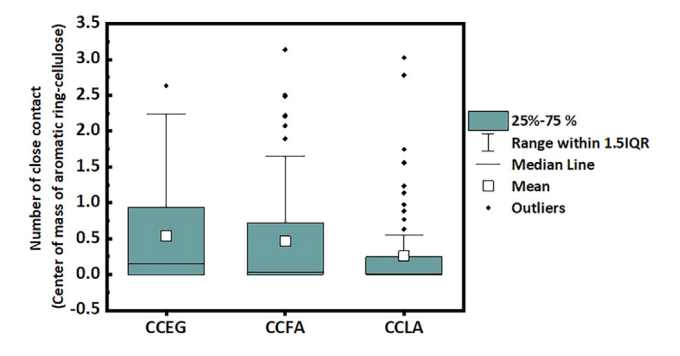


Fig. 11. Average number of close contacts of center of mass of aromatic ring to atoms of cellulose in different DESs.

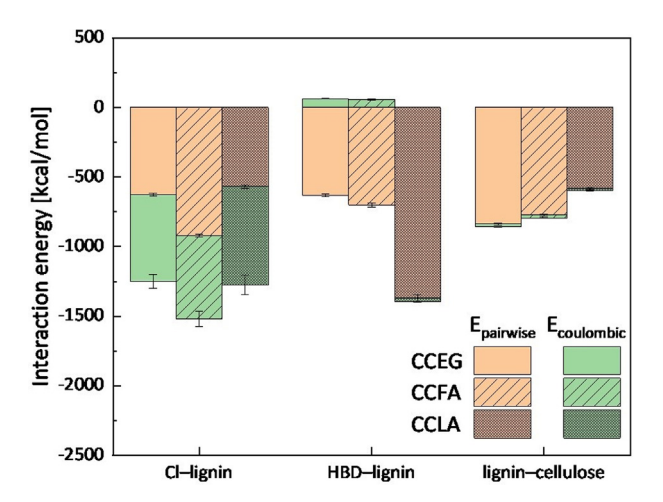
faces of cellulose. Lindner et al. found that based on explicit-water simulations lignin prefers to associate with hydrophobic surfaces of cellulose [34]. However, such a preference does not exist for any of the three DESs studied here. Instead, lignin has more close contacts with cellulose's hydrophilic surface (Fig. 12). Among the three DESs, CCLA shows the greatest ability to prevent the aromatic rings of lignin from associating with cellulose's hydrophobic surfaces. The different behavior of lignin in water versus DESs indicates that DESs effectively disrupt the dominant mechanism of association between cellulose and lignin, and thus help to separate lignin from cellulose in biomass during pretreatment.

Fig. 13 shows the interaction energies for lignin–cellulose and lignin–DES. The highest interaction energy for lignin–cellulose was observed with CCEG, while the lowest was observed with CCLA. This further confirms the ability of CCLA to interrupt the adhesion between lignin and cellulose. Similar to the thermodynamics of chloride–lignin in the solvent system for lignin only (Fig. 8), the chloride–lignin interaction energy in CCFA is also the highest among the three DESs regardless of the size of the lignin model molecule, which is also consistent with the number of H-bonds between chloride ion and lignin found in CCFA (Fig. 5d). This explains why CCFA is still able to reduce the number of close contacts of lignin with cellulose substantially, although formic acid as an HBD is not as strong as lactic acid in terms of competing with H-bonds in lignin and the cellulose–lignin bulk.

#### 4. Discussion

#### 4.1. Local molecular arrangements in DESs

The MD simulation results reveal that the type of HBD in a DES strongly affects the local molecular arrangement. When an HBD has more oxygen atoms per molecule especially for carboxylic acids, the H-bond network tends to be denser, as more H-bonds are generated in HBD-HBD interactions (see Fig. S4 in the Supporting Information). In CCEG, H-bonds mainly result from HBD-anion interactions, whereas in CCFA or CCLA, HBD-HBD interactions are the source of the majority of the H-bonds. In CCFA and CCLA, aggregation occurs among the carboxylic acids, which leads to weaker interactions between chloride anions and the HBDs. In this case, only small amounts of chloride anion can approach the acids. In the meantime, carboxylic acid complexes would slow down the diffusion of free anions, which makes anions remain bound to choline cation via either hydrogen bonding with hydroxyl groups or electrostatic forces with nitrogen atoms. Similar phenomena were found in meline [29], in which chloride anion was found to undergo intense hydrogen bonding with choline cation due to the formation of malonic acid aggregates. Consequently, two different types of complex structure are formed in the three DESs:



**Fig. 13.** Interaction energy (pairwise and long-range Coulombic) for Cl-lignin, HBD-lignin, and lignin-cellulose.

[Cl (EG)]<sup>-</sup> complexes predominate in CCEG, while carboxylic acid dimers predominate in CCFA and CCLA. The occurrence of such complexes can also be corroborated by the unique distributions in SDF centered around choline cation (Fig. 3). Specifically, the distributions of chloride anion and ethylene glycol were found to overlap with one another (Fig. 3a), while a staggered arrangement was observed for chloride anion and carboxylic acids (Fig. 3b&3c).

#### 4.2. Role of HBD and chloride ion in lignin dissolution

SASA values and the number of lignin-lignin H-bonds have been used to characterize lignin structural changes [31,34]. Both GG dimer and Adler lignin were simulated to study how lignin behaves differently in a DES. For a model lignin dimer, the main lignin-lignin interaction is intermolecular due to its higher flexibility in the solvent endowed by its smaller size and higher mobility. Thus, the SASA of GG would change due to the influence of Hbonds from solvent molecules and other GG molecules. In contrast, intramolecular H-bonds are more common in Adler lignin due to the more branched and complex structure with various interlinkages. When interacting with solvent molecules, Adler lignin can impose significant steric hindrance that impedes solvent molecules from hydrogen bonding with oxygen atoms in lignin. On the other hand, once solvent molecules bind to hydroxyl groups in lignin. they might be able to pre-position the lignin molecules and prevent them from aggregating via intramolecular hydrogen bonding.

HBDs play a key role in lignin dissolution and bond cleavage in a choline chloride-based DES [6]. During lignin extraction, the HBDs

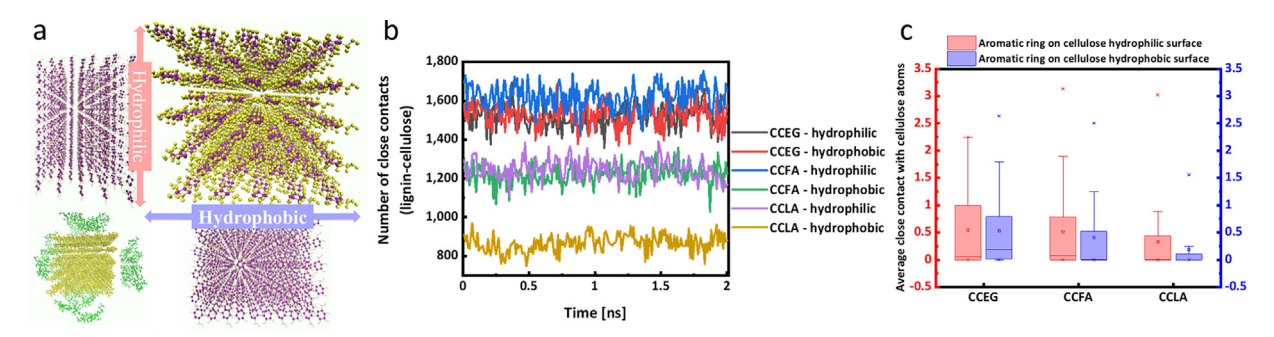


Fig. 12. (a) Diagram of both hydrophilic and hydrophobic surfaces of cellulose. (b) Average number of close contacts of center of mass of aromatic ring to atoms of cellulose on both hydrophilic and hydrophobic surfaces in different DESs. (c) Number of close contacts of lignin–cellulose on both hydrophilic and hydrophobic surfaces in different DESs.

ideally would be initially positioned around the interunit linkages of lignin to supply the protons necessary for further acid-catalyzed cleavage. The β-O-4 bond of lignin is considered to be the most vulnerable interunit linkage in lignin [35]. One possible mechanism of proton-induced cleavage of β-O-4 bonds involves protonation of a benzylic carbon  $(C\alpha)$  followed by dehydration and formation of the carbocation and further bond cleavage via different routes [36]. HBDs can provide the protons necessary for the cleavage of β-O-4 interunit linkages. Depending on its size and composition, the HBD can also influence the number of hydrogen bonds formed with lignin and the optimal sites on lignin for interaction with the solvent. In CCEG, ethylene glycol molecules preferentially occupy  $\alpha$ -OH rather than  $\gamma$ -OH in lignin based on the average number of H-bonds per OH group (Table S3). Prior studies also reported that  $\alpha$ -OH is a preferred site for the interaction of halide anions (e.g., Br<sup>-</sup>, Cl<sup>-</sup>) [6,14] in ionic liquids with lignin. Therefore, [Cl (EG)] complexes could get involved in the cleavage of  $\beta$ -O-4 bonds. There would also be an atom exchanged between [Cl (EG)] and lignin during bond cleavage. When a carbocation intermediate is formed during the cleavage of a β-O-4 bond, chloride from the complexes might bind to the carbocation immediately to protect such an intermediate from further cleavage [37]. A prior study on lignin extraction using CCEG with a varying molar ratio of HBD to HBA suggested that chloride ion could play a role in stabilizing the carbocation formed during  $\beta$ -O-4 linkage [12]. With the anion's protection, the extracted lignin would have more preserved β-O-4 linkages after the pretreatment. The finding for [Cl (EG)] here further confirms the feasibility of binding of chloride anion to the carbocation and the role of the anion in preserving β-O-4 bonds.

In CCFA and CCLA, carboxylic acid dimers appear around  $\gamma$ -OH in lignin (Fig. 6d). Such dimers play a role in providing or accepting protons in hydrogen bonding interactions with lignin molecules. The hydroxyl groups in lignin might be trapped within the dimers and further blocked from contacting other oxygen atoms in lignin. The dimers, especially lactic acid dimers, are larger and thus prefer to interact with hydroxyl groups in lignin that have less steric hindrance, such as  $\gamma$ -OH and Ar-OH. Because carboxylic acid molecules and anions have the same optimal sites in lignin, they might cooperate with each other to attack  $\gamma$ -OH from aliphatic chains. In a recent experimental study of using CCLA for biomass pretreatment, Smink et al. [38] found that the presence of chloride anion would accelerate the delignification efficiency of lactic acid. Our simulations suggest that the mechanism is more likely to be synergistic effects of chloride anion and HBD acting on the same site in lignin. In addition, the local arrangement of chloride ions can also vary in response to the complexation of carboxylic acids. As mentioned previously, supermolecules, especially lactic acid dimers, can be advantageous in opening lignin's structure and reducing self-aggregation while making chloride anion more accessible to lignin.

#### 4.3. Adsorption behavior of lignin on cellulose surface in DESs

The adsorption of lignin on cellulose is presumed to be surface-dependent [9]. On the hydrophilic surface of cellulose, adsorption is expected to be hydrogen-bond-driven [9,39]. An ideal HBD would be able to bind with as many oxygen atoms in lignin as possible to weaken lignin-cellulose hydrogen bonding interactions as well as disrupt lignin-lignin H-bonds. As a result, lignin would be dissociated from cellulose surfaces and also be prevented from self-aggregation. In this respect, CCLA can disrupt more lignin-cellulose and lignin-lignin H-bonds than CCFA and CCEG. Compared to CCLA, a greater number of lignin-cellulose close

contacts on hydrophilic surfaces are observed with CCFA (Fig. 12b). This observation implies that CCFA does not provide sufficient H-bond strength to separate lignin from cellulose on the hydrophilic surface. On the hydrophobic surfaces of cellulose, most of the area is covered by the glucopyranose rings, so hydrogen bonding is not the dominant force for lignin-cellulose interactions. Instead, the hydrophobic nature of lignin makes it tend to adhere to the hydrophobic surfaces of cellulose (especially in water) with the aromatic ring being parallel to the surface [33]. When a lignindissolving DES is used, this affinity can be disrupted by reducing the occurrence of the aromatic structures of lignin being adhered to the hydrophobic surfaces of cellulose. Compared to the hydrophilic surfaces, the number of close contacts of lignin (calculated by the way of the center of mass of its aromatic rings) on the hydrophobic surfaces is even smaller (Fig. 12c), with the narrowest distribution being observed with CCLA. Among the three HBDs, we found that lactic acid not only disrupted more lignin-lignin hydrogen bonds, but also worked best for reducing lignin-cellulose contacts on both hydrophilic and hydrophobic surfaces (Figs. 9 and 11). Formic acid is not as good as lactic acid at preventing lignin deposition on the surface of cellulose; however, it can noticeably reduce lignin-cellulose contacts and impede the self-aggregation of lignin. In contrast to CCLA and CCFA, CCEG shows less potential to disrupt lignin-cellulose association. These findings are in agreement with those revealed by experimental studies. Zhang et al. found that CCLA-pretreated corn cob contained less lignin and had higher cellulose crystallinity index (CrI) than the CCEGpretreated one [40]. Similarly, Chen et al. reported that CCLA can remove about three times more lignin from switchgrass than CCEG under the same pretreatment condition [11,12]. CCLA was also found to remove more lignin and hemicellulose from corn stover than CCFA, leading to much more increased CrI of corn stover cellulose [41,42].

#### 5. Conclusions

This molecular dynamics simulation study reveals the role of common solvent supermolecular complexes of three deepeutectic solvents (DESs) in the dissolution of lignin and characterizes the structural changes of lignin as well as the disassociation of cellulose-lignin complexes in DESs. The three DESs use choline chloride as a hydrogen bond acceptor paired with ethylene glycol, formic acid, or lactic acid as a hydrogen bond donor (HBD). The HBD plays an important role in the solvent's structure, as it forms complexes with anions or itself, depending on the nature of the HBD. The HBD-based supermolecular complexes can further affect the solvation of lignin by changing the density of the hydrogen bond network and disrupting lignin-lignin hydrogen bonds. Moreover, HBD complexes and chloride anion have different preferential sites on lignin. These mechanisms account for DESs' performance in lignin dissolution and extraction. The mechanistic insights obtained from this work provide guidance on the rational design of DESs for biomass pretreatment, lignin extraction, and lignin valorization, and are a step on the path to sustainable pulping and biorefining.

#### **CRediT authorship contribution statement**

**Qianwei Li:** Conceptualization, Methodology, Investigation, Formal analysis, Writing – original draft. **Yuan Dong:** Methodology, Writing – review & editing. **Karl D. Hammond:** Writing – review & editing. **Caixia Wan:** Conceptualization, Supervision, Project administration, Writing – review & editing, Funding acquisition.

#### **Declaration of Competing Interest**

The authors declare that they have no known competing financial interests or personal relationships that could have appeared to influence the work reported in this paper.

#### Acknowledgements

Q. Li and C. Wan acknowledge the support from the National Science Foundation (Award No. 1933861) and USDA National Institute of Food and Agriculture (Award No. 2021-67021-34504). Y. Dong acknowledges the support from the National Natural Science Foundation of China (Award No. 52006050). The computation for this work was performed on computing infrastructure provided in part by Research Computing Support Service at University of Missouri and in part by the National Science Foundation (Award No. 1429294).

#### **Author contributions**

The manuscript was written through contributions of all authors. All authors have given approval to the final version of the manuscript.

#### Appendix A. Supplementary material

Supplementary data to this article can be found online at https://doi.org/10.1016/j.molliq.2021.117779.

#### References

- [1] N. Fitzgerald, A. Bailey, Moving beyond drop-in replacements: Performance-advantaged biobased chemicals, Department of Energy, Office of Energy Efficiency & Renewable Energy, Bioenergy Technologies Office, Washington, DC. Workshop Summary Report, 2018. URL: https://www.energy.gov/sites/prod/files/2018/06/f53/Performance-Advantaged%20Biobased%20Chemicals%20Workshop%20Report.pdf
- 2] J.G. Lynam, N. Kumar, M.J. Wong, Bioresource Technol. 238 (2017) 684.
- [3] D.J.G.P. van Osch, L.J.B.M. Kollau, A. van den Bruinhorst, S. Asikainen, M.A.A. Rocha, M.C. Kroon, Phys. Chem. Chem. Phys. 19 (2017) 2636.
- [4] M. Francisco, A. van den Bruinhorst, M.C. Kroon, Angew. Chem. Int. Ed. 52 (2013) 3074.
- [5] M. Frauenkron, J.-P. Melder, G. Ruider, R. Rossbacher, H. Höke, Environ. Protect. 421 (2012) 8.

- [6] Z. Chen, A. Ragauskas, C. Wan, Ind. Crops Prod. 147 (2020) 112241.
- [7] Q. Xia, Y. Liu, J. Meng, W. Cheng, W. Chen, S. Liu, Y. Liu, J. Li, H. Yu, Green Chem. 20 (2018) 2711.
- [8] H. Ji, P. Lv, Green Chem. 22 (2020) 1378.
- [9] S. Besombes, K. Mazeau, Plant Physiol. Biochem. 43 (2005) 299.
- [10] M. Al Ameri, Deep Eutectic Solvent Pretreatment for Enhancing Biochemical Conversion of Switchgrass. Thesis, University of Missouri, 2017.
- [11] Z. Chen, X. Bai, A Lusi, C. Wan, ACS Sustain, Chem. Eng. 6 (2018) 12205.
- [12] Z. Chen, Y. Sun, C. Wan, Cellulose 26 (2019) 9439.
- [13] S. Jia, B.J. Cox, X. Guo, Z.C. Zhang, J.G. Ekerdt, Ind. Eng. Chem. Res. 50 (2011) 849.
- [14] Y. Zhang, H. He, K. Dong, M. Fan, S. Zhang, RSC Adv. 7 (2017) 12670.
- [15] Y. Zhang, F. Huo, Y. Wang, Y. Xia, X. Tan, S. Zhang, H. He, Front. Chem. 7 (2019) 78.
- [16] T. Zhang, X. Li, L. Guo, Langmuir 33 (2017) 11646.
- [17] T. Zhang, X. Li, X. Qiao, M. Zheng, L. Guo, W. Song, W. Lin, Energy Fuels 30 (2016) 3140.
- [18] S.C. Rismiller, M.M. Groves, M. Meng, Y. Dong, J. Lin, Fuel 215 (2018) 835.
- [19] Biovia Materials Studio: An Integrated, Multi-Scale Modeling Environment, Dassault Systèmes, San Diego, 2011.
- [20] W. Jorgensen, D.S. Maxwell, J. Tirado-Rives, J. Am. Chem. Soc. 118 (1996) 11225.
- [21] M. Gilmore, L.M. Moura, A.H. Turner, M. Swadźba-Kwaśny, S.K. Callear, J.A. McCune, O.A. Scherman, J.D. Holbrey, J. Chem. Phys. 148 (2018) 193823.
- [22] B. Doherty, O. Acevedo, J. Phys. Chem. B 122 (2018) 9982.
- [23] A.I. Jewett, Z. Zhuang, J.-E. Shea, Biophys. J. 104 (2013) 169.
- [24] Q. Liu, X. Zhao, D. Yu, H. Yu, Y. Zhang, Z. Xue, T. Mu, Green Chem. 21 (2019) 5291
- [25] S. Plimpton, J. Comput. Phys. 117 (1995) 1.
- [26] W. Humphrey, A. Dalke, K. Schulten, J. Mol. Graph. 14 (1996) 33.
- [27] M. Brehm, B. Kirchner, J. Chem. Inf. Model. 51 (2011) 2007.
- [28] C. D'Agostino, R.C. Harris, A.P. Abbott, L.F. Gladden, M.D. Mantle, Phys. Chem. Chem. Phys. 13 (2011) 21383.
- [29] S.L. Perkins, P. Painter, C.M. Colina, J. Chem. Eng. Data 59 (2014) 3652.
- [30] M. Losada, H. Tran, Y. Xu, J. Chem. Phys. 128 (2008) 014508.
- [31] M.D. Smith, B. Mostofian, X. Cheng, L. Petridis, C.M. Cai, C.E. Wyman, J.C. Smith, Green Chem. 18 (2016) 1268.
- [32] Y. Zhu, J. Yan, C. Liu, D. Zhang, Biopolymers 107 (2017) e23022.
- [33] S. Besombes, K. Mazeau, Plant Physiol. Biochem. 43 (2005) 277.
- [34] B. Lindner, L. Petridis, R. Schulz, J.C. Smith, Biomacromolecules 14 (2013) 3390.
- [35] W. Boerjan, J. Ralph, M. Baucher, Annu. Rev. Plant Biol. 54 (2003) 519.
- [36] W. Schutyser, T. Renders, S. Van den Bosch, S.F. Koelewijn, G.T. Beckham, B.F. Sels, Chem. Soc. Rev. 47 (2018) 852.
- [37] Z. Chen, X. Bai, A Lusi, H. Zhang, C. Wan, ACS Sustain. Chem. Eng. 8 (2020) 9783
- [38] D. Smink, A. Juan, B. Schuur, S.R.A. Kersten, Ind. Eng. Chem. Res. 58 (2019) 16348.
- [39] J.V. Vermaas, M.F. Crowley, G.T. Beckham, ACS Sustain. Chem. Eng. 7 (2019)
- [40] C.-W. Zhang, S.-Q. Xia, P.-S. Ma, Bioresour. Technol. 219 (2016) 1.
- [41] G.-C. Xu, J.-C. Ding, R.-Z. Han, J.-J. Dong, Y. Ni, Bioresour. Technol. 203 (2016)
- [42] Z. Chen, C. Wan, Bioresour. Technol. 250 (2018) 532.